

# Inland Thinning of Pine Island Glacier, West Antarctica

Andrew Shepherd,<sup>1\*</sup> Duncan J. Wingham,<sup>1</sup> Justin A. D. Mansley,<sup>1</sup>  
Hugh F. J. Corr<sup>2</sup>

The Pine Island Glacier (PIG) transports 69 cubic kilometers of ice each year from ~10% of the West Antarctic Ice Sheet (WAIS). It is possible that a retreat of the PIG may accelerate ice discharge from the WAIS interior. Satellite altimetry and interferometry show that the grounded PIG thinned by up to 1.6 meters per year between 1992 and 1999, affecting 150 kilometers of the inland glacier. The thinning cannot be explained by short-term variability in accumulation and must result from glacier dynamics.

The West Antarctic Ice Sheet (WAIS) contains enough water to raise global sea level by ~5 m (1) if the ice were to melt into the ocean. The Pine Island Glacier (PIG) (Fig. 1) has the largest discharge (75 Gt year<sup>-1</sup>) of all WAIS ice streams (2). A bedrock topography that deepens inland and the absence of an extensive ice shelf have motivated theoretical arguments (3–7) about the behavior of grounding lines of this type, and encouraged speculation that a retreat of PIG could accelerate mass discharge from the WAIS interior (8–11). Evidence of dynamic fluctuations in the inland PIG is therefore of considerable interest. Satellite radar interferometry observations (12) have shown that the PIG grounding line retreated 5 km inland between 1992 and 1996. Here we show that this grounding line retreat is associated with an ice dynamic

fluctuation affecting a large fraction of the inland glacier.

We used European Remote-Sensing (ERS) satellite altimetry to determine the rate of change of ice thickness of the entire PIG drainage basin between 1992 and 1999, and ERS satellite interferometry to determine its relation to the flow of ice within the fast-moving section. We differenced altimeter range measurements at individual crossing points of the satellites' ground tracks to determine elevation changes within the basin, which fell completely inside the instruments' region of coverage. We combined range measurements from ERS-1 and ERS-2 35-day orbit repeat cycles to form (13) a time series of elevation change at each individual crossing point (Fig. 2). Using this time series, we calculated (13) the 7-year rate of elevation change at each point within the PIG drainage basin (Fig. 3). To establish the relation of the elevation change to the ice velocity, we mapped the ice velocity using satellite radar interferometry (Fig. 3). A previous study determined the ice velocity at the upper tribu-

aries (14). We used pairs of ascending and descending orbit, ERS synthetic aperture radar (SAR) data recorded between 1994 and 1996, with temporal baselines of 1 and 3 days, to measure the complete range of ice speeds from the slow interior to the fast-moving downstream ice (15).

Between 1992 and 1999, the interior of the drainage basin thinned at a rate of ~0.1 m year<sup>-1</sup>. This thinning, which extends into the neighboring Thwaites Glacier drainage basin, is comparable (16) to the expected variability in snowfall. It may simply reflect a short-term accumulation shortfall. However, a more rapid thinning also occurred coincident with fast ice motion (Fig. 3). Thinning of  $1.6 \pm 0.2$  m year<sup>-1</sup> occurred near the grounding line, consistent with the grounding line retreat observed previously (12). The thinning was reduced inland (Fig. 4B) but was discernible 150 km upstream from the grounding line. We detected no appreciable change in the rate of ice thinning during the period of satellite observations.

PIG is fed by tributary ice flows (14) that originate deep in the ice sheet interior and converge ~175 km inland to form the central trunk of the fast-flowing outlet glacier. Estimates of the ice deformation velocity (14) suggest that these glaciers are sliding over their beds along each tributary ~50 km upstream of the central trunk. The trunk is bounded roughly by the 200 m year<sup>-1</sup> velocity contour (Fig. 3). The thinning is largely confined to the trunk (Fig. 3) and does not affect the sliding ice of the tributaries. New radar echo soundings of PIG [(17), redrawn in Fig. 4A] provide an estimate of the ice thickness. The trunk of PIG is seated within a subglacial trough that is over 500 m deeper than the bed beneath the easternmost tributaries (Fig. 4A), which may explain the pattern of ice thinning. Interpolating the observed thinning

<sup>1</sup>Centre for Polar Observation & Modelling, Department of Space and Climate Physics, University College London, 17 Gordon Street, London, WC1H 0AH, UK. <sup>2</sup>British Antarctic Survey, High Cross, Madingley Road, Cambridge CB3 0ET, UK.

\*To whom correspondence should be addressed. E-mail: aps@mssl.ucl.ac.uk

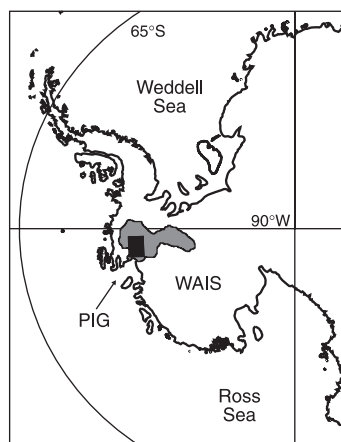


Fig. 1. Map of West Antarctica, showing the location of the PIG drainage basin (gray) and the downstream region shown in Fig. 3 (black).

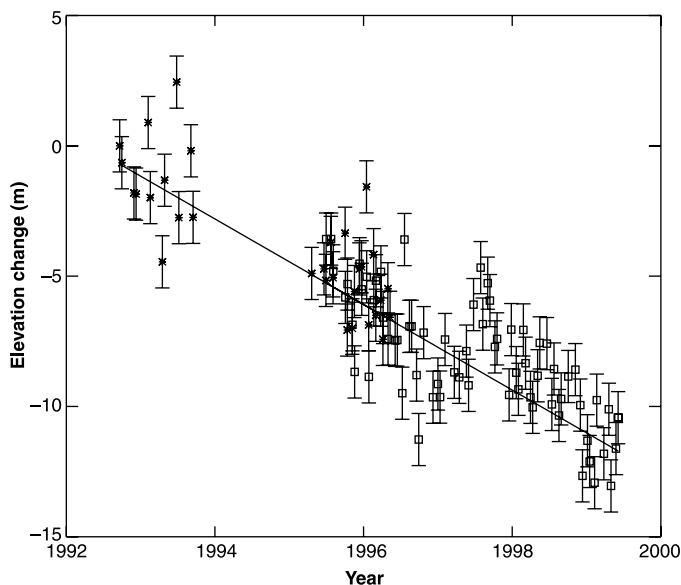


Fig. 2. The change in surface elevation 13 km upstream of the grounding line of PIG between 1992 and 1999, observed by the ERS-1 (stars) and ERS-2 (squares) satellite altimeters. The 6-month period of simultaneous operation permitted cross-calibration of the altimeters. Data gaps are the result of instrument operations. The location of this time series is shown as a colored dot highlighted with a solid black perimeter in Fig. 3.

## REPORTS

over the glacier trunk (Fig. 3), the average rate of thinning is  $0.042 \pm 0.005\%$  year<sup>-1</sup>. However, much of the bed lies below sea level (Fig. 4A) (at its deepest section, the hydrostatic overburden of the trunk is only 535 m of ice).

Although the evolution of the thinning remains uncertain, if the trunk continues to lose mass at the present rate it will be entirely afloat within 600 years (18).

We examined the possibility that the thin-

ning is the result of short-term changes in the surface mass balance. The elevation change of the glacier trunk ( $-0.75$  m year<sup>-1</sup> in Fig. 3) is, on average, almost an order of magnitude greater than expected fluctuations in snowfall [ $9.3$  cm year<sup>-1</sup> in (16)]. Interannual changes in katabatic winds, which may be spatially correlated with the pattern of ice flow, could enhance the short-term surface ablation of the glacier. However, the thinning is up to 13 times larger than the variability we estimate (19) from this source. The thinning we observe is far greater than any reasonable fluctuation in the surface mass balance. Rapid variations in the mass supply from the interior are unlikely, and there is no evidence of thinning in either the upper glacier tributaries or the ice sheet interior. The rate of thinning in the future depends on how the velocity of the trunk adjusts to the long-term accumulation mean. In consequence, the time scale for the thinning process is that of an ice dynamic fluctuation and not that of mass supply from the atmosphere.

Potential sources of fluctuations in ice stream velocity are numerous. According to theoretical arguments (6, 7, 20–23), ice dynamic mechanisms that could be responsible for the thinning provide a variety of time scales ranging from  $10^1$  to  $10^4$  years. Processes that continue for millennia, such as thermally regulated oscillations in basal lubrication (20), could affect a substantial fraction of the ice sheet. There is speculation that such behavior is typical of ice streams (7). However, simple computer models predict that upstream thinning is associated with downstream thickening and grounding line advance, which are not seen in the data (Fig. 4B). The shortest lived events ( $10^1$  to  $10^2$  years), such as glacier surges (23), should be resolved by the time series of elevation change. However, we detect no change in the rate of ice thinning across the glacier over a 7-year period (Fig. 2). Processes that could affect the equilibrium state of the glacier at intermediate time scales ( $10^2$  to  $10^3$  years) are therefore the most likely. The thinning could be largely due to increased velocities within the central trunk. There is some evidence (21) for the existence of a more extensive ice shelf than at present (Fig. 4A), the collapse of which may have precipitated such a response. Computer simulations (6, 22) of this type of disturbance, albeit of simpler dynamical situations than that apparent in PIG (Fig. 4A), predict a pattern of thinning similar to that in Fig. 4B. A more detailed understanding of PIG's departure from equilibrium flow will require an understanding of its particular stream mechanics.

We estimate from Fig. 3 that the present rate of thinning is reducing the mass of PIG by  $3.9 \pm 0.9$  Gt year<sup>-1</sup>, or  $\sim 5\%$  of the mass flux across the grounding line, which is

**Fig. 3.** The rate of elevation change of the lower 200 km of PIG between 1992 and 1999 (colored scale) registered with a map of the ice surface speed (gray scale). The colored dots are located at crossing points of the ERS orbit ground tracks and have an area equal to the radar altimeter footprint. The velocity field is restricted to regions of overlap between ascending and descending ERS SAR coverage. Also shown are the trajectory of a recent radar echo flight (red dashed line) and the boundary we chose to delimit the glacier trunk from the remainder of the drainage basin (black dashed line). The trunk is bounded laterally by the 200 m year<sup>-1</sup> velocity contour and streamwise by the grounding line (lower solid black line) located by Rignot (12) and the intersection of the easternmost tributaries, which coincide roughly with a deep bedrock trough (Fig. 4A). The greatest elevation change is adjacent to the grounding line, and the thinning is concentrated over fast-flowing ice. Changes beyond the region of fast flow were much smaller, although there is some evidence that the tributary joining the glacier at the southern edge of the grounding line is also thinning. We calculate the mean rate of elevation change of the glacier trunk to be  $-0.75 \pm 0.07$  m year<sup>-1</sup> and that of the remainder of the basin (including that not shown here) to be  $-0.11 \pm 0.01$  m year<sup>-1</sup>.

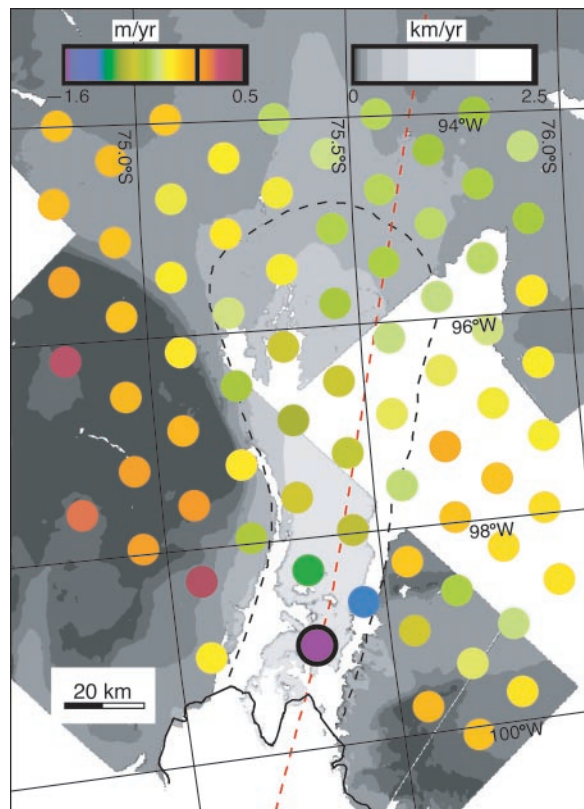
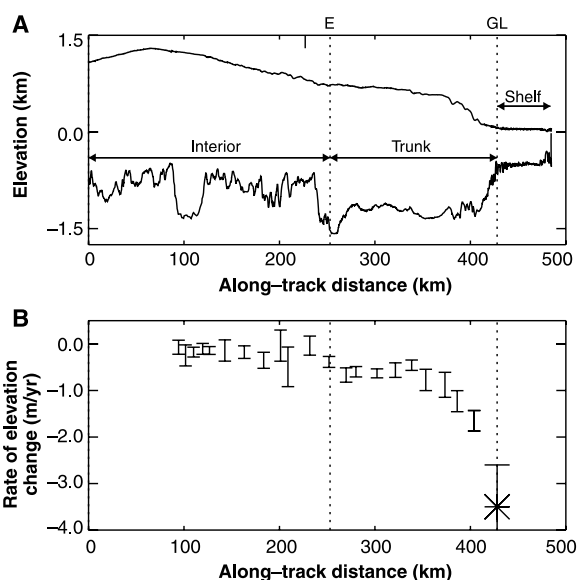


**Fig. 4.** (A) Bedrock and surface elevation along PIG from airborne ice-penetrating radar (17). The grounding line (GL) lies within a ( $\sim 30$  km) zone of near-buoyancy where small changes in ice thickness result in large GL migration. Upstream of this region there is a deep subglacial trough that holds the central trunk of the PIG. The trunk boundary is coincident with the intersection of the flight trajectory and the locus of fast flow described in Fig. 3. The easternmost edge of Fig. 3 is also marked (E). The glacier develops a driving stress in excess of 100 kPa in surmounting the bedrock trough, and the associated upstream thickening appears to determine the location of the present grounding line. (B) Rate of elevation change (1992–1999) measured by ERS radar altimeter at discrete locations along the same transect. Also shown is the value determined by Rignot (12) for the thinning (1992–1996) at the grounding line. The thinning is largely confined to the region of high driving stress, suggesting that the progress of retreat may be controlled by the dynamics of this section of PIG.



equivalent to 0.01 mm year<sup>-1</sup> of eustatic sea level rise. If the entire grounded section of PIG were lost to the ocean, we estimate the net contribution to eustatic sea level to be 6 mm (18). Both of these are small in comparison with other expected changes in sea level (1). On the other hand, if sufficiently prolonged, the present thinning could affect the flow of what is now slow-moving ice in the interior, increasing the volume of rapidly drained ice (10).

References and Notes

1. R. Warrick, C. Le Provost, M. Meier, J. Oerlemans, P. Woodworth, in *Climate Change 1995: The Science of Climate Change* (Cambridge Univ. Press, Cambridge, 1996), pp. 359–405.
2. C. R. Bentley, M. B. Giovinetto, in *Proceedings of the International Conference on the Role of Polar Regions in Global Change* (Univ. of Alaska, Fairbanks, AK, 1991), pp. 481–488. The authors obtained 26 Gt year<sup>-1</sup> for the ice discharge flux of PIG. We used the improved estimate of 75 Gt year<sup>-1</sup> determined by Rignot *et al.* (24).
3. J. Weertman, *J. Glaciol.* **13**, 3 (1974).
4. R. H. Thomas, *J. Glaciol.* **24**, 167 (1979).
5. V. Barillon, D. R. Macayeal, *J. Glaciol.* **39**, 131 (1993).
6. C. J. Van der Veen, *Quat. Res.* **24**, 257 (1985).
7. R. C. H. Hindmarsh, *Ann. Glaciol.* **23**, 105 (1996).
8. J. H. Mercer, *Nature* **271**, 321 (1978).
9. T. J. Hughes, *J. Glaciol.* **27**, 518 (1981).
10. D. Lindstrom, T. J. Hughes, *Antarct. J. U.S.* **19**, 56 (1984).
11. M. Oppenheimer, *Nature* **393**, 325 (1998).
12. E. J. Rignot, *Science* **281**, 549 (1998).
13. We followed the method described (16) in forming time series at crossovers of the orbit ground tracks. We examined trends in the backscattered power throughout the basin. We detected no significant correlation at any scale and applied no empirical correction (16) for variation in the ratio of surface-to-volume scattering. Because the crossover locations do vary in detail with time, the elevations were corrected for surface slope (25) with an interferometrically derived elevation model of the basin. The surface slope was less than 1.1° ± 0.1° all over and the mean relocation distance for altimeter footprints was 1.2 ± 0.1 km (~12.5% of the footprint diameter). The associated height correction does not affect calculations of elevation change. The variability of the elevation time series linear trends was ~0.3 m year<sup>-1</sup>, due in part to measurement error and in part to accumulation fluctuations (16).
14. M. D. Stenooin, C. R. Bentley, *J. Geophys. Res.* **105**, 21761 (2000).
15. We differenced pairs of ERS repeat pass interferograms to determine the ice surface speed in the look direction of the SAR (26–28). When pairs of interferograms were not available, the topographic signal was separated from the velocity signal with a coarse resolution digital elevation model. The surface velocity vector was calculated with measurements of speed in independent look directions (28). We mapped 26% (~42,000 km<sup>2</sup>) of the PIG drainage basin, or 48% of the region north of 76.5°S (which includes the vast majority of the glacier and tributary network), using a combination of ascending and descending (49 and 32% of the basin, respectively) SAR scenes. To obtain the interferometer baseline, we combined ice sheet balance velocities (29) for the slow-moving interior, feature-tracked velocities close to the grounding line, and surface elevation tie-points (30). The principal error in the velocity arose from the inadequate distribution of control points. The SD of velocity differences between overlapping images forming the mosaic was ~60 m year<sup>-1</sup>. (Long wavelength errors may also be present but are not relevant to the work described here).
16. D. J. Wingham, A. J. Ridout, R. Scharroo, R. J. Arthern, C. K. Shum, *Science* **282**, 456 (1998).
17. D. G. Vaughan *et al.*, *Antarct. Res. Ser.* **77**, 236 (2001).

18. The areal extent of the fast-flowing glacier is ~5300 km<sup>2</sup>, or ~3% of the drainage basin. From the data in Fig. 4A, we estimate the volume of ice overburden to be ~2100 km<sup>3</sup> of ice (that is, ~6 mm of eustatic sea level). At an average rate of thinning (Fig. 3) of 0.75 m year<sup>-1</sup>, this volume will be removed in 527 years.
19. Katabatic winds are gravity-driven air flows (31). We estimated the interannual variability of wind speed and air temperature from coarse resolution reanalysis fields. We estimated the variability of the annual sublimation rate of PIG to be 0.13 m year<sup>-1</sup> water equivalent using the empirical equation of Bintanja (32). We also estimated the variability in erosion due to drifting snow, using the formula of Budd (33), and this was negligible. Although old samples collected from locations close to the grounding line of PIG (34) indicate that the surface density may be closer to that of ice (917 kg m<sup>-3</sup>) than snow (350 kg m<sup>-3</sup>), assuming a value of 400 kg m<sup>-3</sup> provides an interannual variability of elevation of 0.32 m year<sup>-1</sup>. Assuming that the variability is independent from year to year, the 7-year variability of thickness due to ablation is 0.12 m year<sup>-1</sup>.
20. A. J. Payne, *J. Geophys. Res.* **100**, 4249 (1995).
21. T. B. Kellogg, D. E. Kellogg, *J. Geophys. Res.* **92**, 8859 (1987).
22. R. B. Alley, I. M. Whillans, *J. Geophys. Res.* **89**, 6487 (1984).

23. A. C. Fowler, E. Shiavi, *J. Glaciol.* **14**, 104 (1998).
24. E. Rignot, D. G. Vaughan, M. Schmeltz, T. K. Dupont, D. R. Macayeal, in preparation.
25. J. Bamber, *Int. J. Remote Sens.* **15**, 925 (1994).
26. R. M. Goldstein, H. Engelhardt, B. Kamb, R. M. Frolich, *Science* **262**, 1525 (1993).
27. R. Kwok, M. A. Fahnestock, *IEEE Trans. Geosci. Remote Sens.* **34**, 1 (1996).
28. I. Joughin, R. Kwok, M. Fahnestock, *IEEE Trans. Geosci. Remote Sens.* **36**, 25 (1998).
29. W. F. Budd, R. C. Warner, *Ann. Glaciol.* **23**, 21 (1996).
30. H. A. Zebker, R. M. Goldstein, *J. Geophys. Res.* **91**, 4993 (1986).
31. T. R. Parish, D. H. Bromwich, *Nature* **328**, 51 (1987).
32. R. Bintanja, *Ann. Glaciol.* **27**, 251 (1998).
33. M. R. van den Broeke, R. Bintanja, *J. Glaciol.* **41**, 395 (1995).
34. T. B. Kellogg, D. E. Kellogg, T. J. Hughes, *Antarct. J. U.S.* **20**, 79 (1985).
35. Supported by the UK Natural Environment Research Council. Feature-tracked ice speed data were provided by the Earth Observing System Distributed Active Archive Center at the National Snow and Ice Data Center, University of Colorado, Boulder, CO. Wind speed data were provided by the National Center for Atmospheric Research, Boulder, CO.

14 September 2000; accepted 2 January 2001

# Scale Dependence in Plant Biodiversity

M. J. Crawley\* and J. E. Hurrell

The relationship between the number of species and the area sampled is one of the oldest and best-documented patterns in community ecology. Several theoretical models and field data from a wide range of plant and animal taxa suggest that the slope, *z*, of a graph of the logarithm of species richness against the logarithm of area is roughly constant, with *z* ≈ 0.25. We collected replicated and randomized plant data at 11 spatial scales from 0.01 to 10<sup>8</sup> square meters in Great Britain which show that the slope of the log-log plot is not constant, but varies systematically with spatial scale, and from habitat to habitat at the same spatial scale. Values of *z* were low (0.1 to 0.2) at small scales (<100 square meters), high (0.4 to 0.5) at intermediate scales (1 hectare to 10 square kilometers), and low again (0.1 to 0.2) for the largest scale transitions (e.g., East Berks to all of Berkshire). Instead of one process determining changes in species richness across a wide range of scales, different processes might determine plant biodiversity at different spatial scales.

Understanding the determinants of species richness is central to many questions in both pure and applied ecology. At the largest spatial scales and over the longest time scales, species richness is determined by rates of speciation and extinction (1). At smaller spatial scales and over shorter periods of time, the number of species is determined by the birth, death, and dispersal rates of individuals interacting with populations of competitors, mutualists, and natural enemies (2). In all cases, however, the number of species depends on the area sampled (3–5), the absolute

abundances of the species (4, 6, 7), their spatial patterns (8, 9), and the degree of mixing of species (10, 11). The relationship between species richness and area is particularly important in biodiversity studies because it holds out the prospect of predicting species richness at large scales from data gathered relatively inexpensively at much smaller scales (12, 13). It is conventional to use the power law *S* = *cA<sup>z</sup>* to describe the relationship between species richness *S* and the area sampled *A*. The exponent, *z*, is close to 0.25 for several theoretical models (14–16) and for much field data (1), but there are also data where *z* is greater than 0.25 [e.g., on islands, and at large scales generally (1)], and data where the slope is less than 0.25 [e.g., with smaller, plant-sized quadrats (17–19)].

Two fundamentally different processes

Department of Biology, Natural Environment Research Council Centre for Population Biology, Imperial College, Silwood Park, Ascot SL5 7PY, UK.

\*To whom correspondence should be addressed. E-mail: m.crawley@ic.ac.uk